Stability Analysis of a Diffusive Predator-prey Model with Hunting Cooperation*

Shuhao Wu[1] and Yongli Song[2,†]

Abstract In this paper, we are concerned with the dynamics of a diffusive predator-prey model that incorporates the functional response concerning hunting cooperation. First, we investigate the stability of the semi-trivial steady state. Then, we investigate the influence of the diffusive rates on the stability of the positive constant steady state. It is shown that there exists diffusion-driven Turing instability when the diffusive rate of the predator is smaller than the critical value, which is dependent on the diffusive rate of the prey, and the semi-trivial steady state and the positive constant steady state are both locally asymptotically stable when the diffusive rate of the predator is larger than the critical value. Finally, the nonexistence of nonconstant steady states is discussed.

Keywords Predator-prey model, Hunting cooperation, Stability, Turing bifurcation.

MSC(2010) 35K57, 35B32, 92D25.

1. Introduction

In predator-prey models, functional response illustrates the relationship between prey and predator. Recent efforts have revealed that aggregated predators cooperate with each other in hunting. In [5], Conser *et al.* proposed the following functional response incorporating hunting cooperation

$$f(u(t), v(t)) = \frac{Ce_0uv}{1 + hCe_0uv}, \tag{1.1}$$

where $u(t)$, $v(t)$, C, e_0 and h are the population density of prey at time t, the population density of predator at time t, fraction of prey caught by a predator per encounter, total encounter rate between the two species and handing time per prey respectively, and C, e_0 and h are all positive. Other types of functional response concerning hunting cooperation were introduced in [1,2]. In [13], Ryu *et al.* mathematically investigated the predator-prey model proposed by Conser *et al.* [5], which

involves the functional response (1.1) and takes the nondimensional form

$$
\begin{cases}
\frac{du(t)}{dt} = u(1-u) - \frac{\alpha uv^2}{1+uv}, \\[2mm]
\frac{dv(t)}{dt} = \frac{\beta uv^2}{1+uv} - \gamma v,
\end{cases}
\tag{1.2}
$$

where $\alpha,\ \beta > 0$ illustrate interspecific effects between two species and $\gamma > 0$ stands for the death rate of predator. They analyzed the stability of constant nonnegative equilibria and demonstrated the existence of Hopf, saddle-node and Bogdanov-Takens bifurcations [13].

In fact, animals always move around in order to survive. To model the spatial distribution of animals, it is necessary to introduce diffusion into the population dynamics. Diffusive predator-prey models have been discussed by many mathematicians and have been suggested to exhibit complex dynamics, including Turing patterns [18, 19], nonconstant steady states [4, 11, 20], periodic solutions [20, 23] and travelling waves [6–8]. Recently, there has been a growing interest on diffusive predator-prey models with hunting cooperation. In particular, the predator-prey model with hunting cooperation proposed by Alves and Hilker [1] was extended to include diffusion in [3, 12, 14–17, 21]. Self-diffusion and homogeneous Neumann boundary conditions were considered in [3, 15, 21], where the existence and stability of nonnegative equilibria, definitive boundedness of solutions, Hopf bifurcation and Turing instability were studied and it was shown that spatial patterns occur only when the prey spreads faster than the predator. In [12], Ryu and Ko focused on self-diffusion and homogeneous Dirichlet boundary conditions and investigated the asymptotic behavior of positive solutions when hunting cooperation in predators is strong. In [17], Song *et al.* considered self-diffusion and Allee effect in prey and explored self-diffusion-driven Turing instability under the assumption that the prey spreads slower than the predator. In [16], the existence, stability and Hopf bifurcation of the positive equilibrium were explicitly determined for the original model proposed by Alves and Hilker [1] and the existence and stability of spatial patterns induced by cross-diffusion were theoretically analyzed under the assumption that the prey spreads slower than the predator. In [14], Singh and Banerjee incorporated hunting cooperation into Holling type II functional response and numerically investigated the self-diffusion-driven spatial patterns. On the other hand, Zhang and Zhu considered diffusive predator-prey models with predator interference or foraging facilitation proposed by Berec [2], and studied the dynamical behaviour and pattern formation in [24].

However, there are few studies on the diffusive version of model (1.2). In [22], cross diffusion was introduced into model (1.2) by Yan *et al.*, and it was shown that cross diffusion can give rise to Turing instability and complicated patterns. In this paper, we consider the random nature of diffusion and investigate the modification of model (1.2) that incorporates self-diffusion and homogeneous Neumann boundary

conditions and takes the form

$$
\begin{cases}
\frac{\partial u(x,t)}{\partial t} = d_1 \Delta u + u(1-u) - \frac{\alpha u v^2}{1+uv}, & x \in \Omega, \ t > 0, \\[2mm]
\frac{\partial v(x,t)}{\partial t} = d_2 \Delta v + \frac{\beta u v^2}{1+uv} - \gamma v, & x \in \Omega, \ t > 0, \\[2mm]
\frac{\partial u}{\partial n} = \frac{\partial v}{\partial n} = 0, & x \in \partial\Omega, \ t > 0, \\[2mm]
u(x,0) = u_0(x) \geq 0, \quad v(x,0) = v_0(x) \geq 0, \ x \in \Omega.
\end{cases}
\tag{1.3}
$$

Here, Ω is a bounded domain in $\mathbb{R}^N$, $N \geq 1$, and has a smooth boundary $\partial\Omega$, and $u(x,t)$ and $v(x,t)$ are modified as the population densities of prey and predator respectively, at time t and location x. We are concerned with the impact of self-diffusion on the stability of constant nonnegative steady states.

The remaining parts of the paper are organized as follows. Stability of constant nonnegative steady states are considered in Section 2. Nonexistence of nonconstant steady states is discussed in Section 3. Numerical simulations are provided in Section 4. The last section gives a summary of our main results. Throughout this paper, $\mathbb{N}$ and $\mathbb{N}_0$ are referred to as the set of positive integers and the set of nonnegative integers respectively.

2. Stability of constant steady states

Notice that the diffusion coefficients d_1 and d_2 make no difference to the existence of the constant steady states of system (1.3). Namely, the constant steady states of system (1.3) are the same as those of its associated ordinary differential system (i.e. system (1.2)). Obviously, for any $\alpha, \beta, \gamma > 0$, $E_0(0,0)$ and $E_1(1,0)$ are the steady states of system (1.3). It follows from [13] that for system (1.2), $E_0(0,0)$ is a saddle, while $E_1(1,0)$ is a stable node and is globally asymptotically stable when the positive steady states do not exist. If $\beta > \gamma$ and $0 < \alpha < \frac{4\beta(\beta-\gamma)}{27\gamma^2}$, then there are two positive steady states (u_1^*, v_1^*) and (u_2^*, v_2^*), where $v_j = \frac{\gamma}{(\beta-\gamma)u_j}$, $j = 1, 2$, and $0 < u_1^* < \frac{2}{3} < u_2^*$. Moreover, (u_2^*, v_2^*) is always unstable if it exists, while (u_1^*, v_1^*) is asymptotically stable if $(\gamma, \beta) \in R_1$ and $\alpha_h < \alpha < \frac{4\beta(\beta-\gamma)}{27\gamma^2}$, where

$$
R_1 = \left\{ (\gamma, \beta) \,\middle|\, 0 < \gamma \leq \frac{2}{3}, \ \beta > \gamma \right\} \cup \left\{ (\gamma, \beta) \,\middle|\, \gamma > \frac{2}{3}, \ \gamma < \beta < \frac{3\gamma^2 - \gamma}{3\gamma - 2} \right\}, \quad (2.1)
$$

and

$$
\alpha_h = \frac{\beta(\beta - \gamma)(1 + \beta - \gamma)^2(\beta - \gamma(\beta - \gamma))}{(\beta + \gamma)^3}. \tag{2.2}
$$

For more results on system (1.2), we refer to [13]. In what follows, we investigate whether diffusion affects the stability of the steady states $E_1(1,0)$ and (u_1^*, v_1^*). As for (u_1^*, v_1^*), we consider the conditions $(\gamma, \beta) \in R_1$ and $\alpha_h < \alpha < \frac{4\beta(\beta-\gamma)}{27\gamma^2}$.

Let $0 = \mu_0 < \mu_1 < \mu_2 < \cdots < \mu_k < \cdots$, $k \in \mathbb{N}_0$, denote the eigenvalues of $-\Delta$ in Ω associated with Neumann boundary conditions and (u_*, v_*) denote any constant steady state of system (1.3). Then, the linearization of system (1.3) about

(u_*, v_*) is

$$
\begin{cases}
\frac{\partial u(x,t)}{\partial t} - d_1 \Delta u = \left(1 - 2u_* - \frac{\alpha v_*^2}{(1+u_*v_*)^2}\right) u - \frac{\alpha u_* v_*(2+u_*v_*)}{(1+u_*v_*)^2} v, & x \in \Omega, \ t > 0, \\
\frac{\partial v(x,t)}{\partial t} - d_2 \Delta v = \frac{\beta v_*^2}{(1+u_*v_*)^2} u + \left(\frac{\beta u_* v_*(2+u_*v_*)}{(1+u_*v_*)^2} - \gamma\right) v, & x \in \Omega, \ t > 0, \\
\frac{\partial u}{\partial n} = \frac{\partial v}{\partial n} = 0, & x \in \partial\Omega, \ t > 0.
\end{cases}
\tag{2.3}
$$

The corresponding characteristic equations are

$$
\Lambda_n : \lambda_n^2 + T_n \lambda_n + D_n = 0, \ n \in \mathbb{N}_0,
$$

where

$$
T_n = (d_1 + d_2)\mu_n - \left(1 - 2u_* - \gamma + \frac{\beta u_* v_*(2 + u_* v_*) - \alpha v_*^2}{(1 + u_* v_*)^2}\right),
\tag{2.4}
$$

and

$$
\begin{aligned}
D_n = {} & d_1 d_2 \mu_n^2 - \left(d_2\left(1 - 2u_* - \frac{\alpha v_*^2}{(1+u_*v_*)^2}\right) + d_1\left(\frac{\beta u_* v_*(2+u_*v_*)}{(1+u_*v_*)^2} - \gamma\right)\right)\mu_n \\
& + \left(1 - 2u_* - \frac{\alpha v_*^2}{(1+u_*v_*)^2}\right)\left(\frac{\beta u_* v_*(2+u_*v_*)}{(1+u_*v_*)^2} - \gamma\right) + \frac{\alpha\beta u_* v_*^3(2+u_*v_*)}{(1+u_*v_*)^4}.
\end{aligned}
\tag{2.5}
$$

For any $n \in \mathbb{N}_0$, all roots of Λ_n have negative real parts if and only if $T_n > 0$ and $D_n > 0$.

Next, we discuss the stability of $E_1(1,0)$ and (u_1^*, v_1^*) in the following two subsections respectively.

2.1. Stability of $E_1(1,0)$

Theorem 2.1. *For any $d_1, d_2 \geq 0$, $E_1(1,0)$ is locally asymptotically stable.*

Proof. When $(u_*, v_*) = E_1(1,0)$, we have

$$
T_n = (d_1 + d_2)\mu_n + 1 + \gamma > 0, \ D_n = d_1 d_2 \mu_n^2 + (d_2 + d_1\gamma)\mu_n + \gamma > 0, \ \text{for } n \in \mathbb{N}_0,
$$

which indicate that for any $n \in \mathbb{N}_0$, all roots of Λ_n have negative real parts. This completes the proof. $\qquad\square$

Next, we use the Lyapunov functional method and derive the following theorem for the semi-trivial steady state $E_1(1,0)$.

Theorem 2.2. *Assume that $\beta \leq \gamma$. Then, for any $d_1, d_2 > 0$, any positive solution of system* (1.3) *converges to $E_1(1,0)$ as time increases.*

Proof. We suppose $u > 0$ and $v \geq 0$ and define

$$
V(t) = \beta \int_\Omega \int_1^u \frac{\eta - 1}{\eta} d\eta dx + \frac{1}{2}\alpha \int_\Omega v^2 dx.
$$

Then, a straightforward calculation gives

$$V'(t)$$

$$= \beta \int_\Omega \frac{u-1}{u} u_t dx + \alpha \int_\Omega v v_t dx$$

$$= -\beta d_1 \int_\Omega \frac{|\nabla u|^2}{u^2} dx + \beta \int_\Omega (u-1)\left(1 - u - \frac{\alpha v^2}{1+uv}\right) dx - \alpha d_2 \int_\Omega |\nabla v|^2 dx$$

$$+ \alpha \int_\Omega v^2 \left(\frac{\beta uv}{1+uv} - \gamma\right) dx$$

$$= -\beta d_1 \int_\Omega \frac{|\nabla u|^2}{u^2} dx - \alpha d_2 \int_\Omega |\nabla v|^2 dx - \beta \int_\Omega (u-1)^2 dx - \alpha\beta \int_\Omega \frac{uv^2}{1+uv} dx$$

$$- \alpha(\gamma - \beta) \int_\Omega v^2 dx.$$

Since $\beta \le \gamma$, we see that $V'(t) \le 0$ for $u > 0$ and $v \ge 0$, and $V'(t) = 0 \iff (u,v) = E_1(1,0)$. This, along with Theorem (2.1), proves the theorem. $\qquad\square$

2.2. Stability and bifurcation analysis of (u_1^*, v_1^*)

Theorem 2.3. *Assume that $(\gamma, \beta) \in R_1$ and $\alpha_h < \alpha < \frac{4\beta(\beta-\gamma)}{27\gamma^2}$, where R_1 and α_h are defined by (2.1) and (2.2) respectively.*

(I) *If $d_1 = 0$ and $d_2 \ge 0$, then (u_1^*, v_1^*) is locally asymptotically stable.*

(II) *If $d_1 > 0$, then (u_1^*, v_1^*) is unstable for $0 \le d_2 < \zeta(d_1)$ and locally asymptotically stable for $d_2 > \zeta(d_1)$; moreover, Turing bifurcation occurs at $d_2 = \zeta(d_1)$ provided that $d_1 \ne d_{1,n}$ and Turing-Turing bifurcation occurs at $(d_1, d_2) = (d_{1,n}, \zeta(d_{1,n}))$, where*

$$d_{1,n} = \frac{1}{2}(2 - 3u_1^*)\left(\frac{1}{\mu_n} + \frac{1}{\mu_{n+1}}\right)$$

$$+ \frac{1}{2}\sqrt{(2-3u_1^*)^2\left(\frac{1}{\mu_n} + \frac{1}{\mu_{n+1}}\right)^2 - \frac{4(2-3u_1^*)(\gamma - u_1^*(\beta+\gamma))}{\beta\mu_n\mu_{n+1}}} > 0, \ n \in \mathbb{N},$$
(2.6)

and

$$\zeta(d_1) = \begin{cases} \zeta_1(d_1), \ \text{if } d_1 \ge d_{1,1} > 0, \\[2mm] \zeta_n(d_1), \ \text{if } d_{1,n} \le d_1 < d_{1,n-1} \ \text{for} \ n \ge 2, \end{cases}$$
(2.7)

with

$$\zeta_n(d_1) = \frac{\gamma(\beta - \gamma)(d_1\mu_n - (2 - 3u_1^*))}{d_1\beta\mu_n^2 - \mu_n(\gamma - u_1^*(\beta+\gamma))} > 0, \ n \in \mathbb{N}.$$
(2.8)

Proof. Let $(u_*, v_*) = (u_1^*, v_1^*)$. A direct calculation shows

$$T_0 \begin{cases} < 0 \iff 0 < u_1^* < \frac{\gamma(1+\beta-\gamma)}{\beta+\gamma}, \\[2mm] = 0 \iff u_1^* = \frac{\gamma(1+\beta-\gamma)}{\beta+\gamma}, \\[2mm] > 0 \iff u_1^* > \frac{\gamma(1+\beta-\gamma)}{\beta+\gamma}. \end{cases}$$
(2.9)

When $(\gamma, \beta) \in R_1$ and $\alpha_h < \alpha < \frac{4\beta(\beta-\gamma)}{27\gamma^2}$, we have $u_1^* > \frac{\gamma(1+\beta-\gamma)}{\beta+\gamma}$, which, together with (2.4), (2.9) and the fact that $\frac{\gamma(1+\beta-\gamma)}{\beta+\gamma} > \frac{\gamma}{\beta+\gamma}$, gives

$$T_n \geq T_0 > 0, \text{ for } n \in \mathbb{N}, \tag{2.10}$$

and

$$u_1^* > \frac{\gamma}{\beta + \gamma}. \tag{2.11}$$

Since $0 < u_1^* < \frac{2}{3}$, it is clear that

$$D_0 = \frac{\gamma(\beta - \gamma)(2 - 3u_1^*)}{\beta} > 0. \tag{2.12}$$

By (2.5) and (2.11), we find that if $d_1 = 0$ and $d_2 \geq 0$, then

$$D_n = \frac{-d_2\mu_n\left(\gamma - u_1^*(\beta + \gamma)\right) + \gamma(\beta - \gamma)\left(2 - 3u_1^*\right)}{\beta} > 0, \ n \in \mathbb{N}, \tag{2.13}$$

while if $d_1 > 0$ and $d_2 \geq 0$, then for $n \in \mathbb{N}$,

$$D_n \begin{cases} < 0 \Longleftrightarrow d_2 < \zeta_n(d_1), \\[2mm] = 0 \Longleftrightarrow d_2 = \zeta_n(d_1), \\[2mm] > 0 \Longleftrightarrow d_2 > \zeta_n(d_1), \end{cases} \tag{2.14}$$

where $\zeta_n(d_1)$ is defined by (2.8). Therefore, by using (2.10), (2.12) and (2.13), we can conclude that when $d_1 = 0$ and $d_2 \geq 0$, all roots of Λ_n have negative real parts for any $n \in \mathbb{N}_0$. By (2.8) and (2.11), it is easily shown that

$$\zeta_n(d_1) > 0 \Longleftrightarrow d_1 > \frac{2 - 3u_1^*}{\mu_n}, \tag{2.15}$$

and

$$\zeta_n(d_1) - \zeta_{n+1}(d_1) \begin{cases} > 0 \Longleftrightarrow d_1 > d_{1,n}, \\[2mm] = 0 \Longleftrightarrow d_1 = d_{1,n}, \\[2mm] < 0 \Longleftrightarrow d_1 < d_{1,n}, \end{cases} \tag{2.16}$$

where $d_{1,n}$ is defined by (2.6). Since $\lim\limits_{n\to\infty} \frac{2-3u_1^*}{\mu_n} = 0$, we see that when $d_1 > 0$ and $d_2 = 0$, there exists $n_* \in \mathbb{N}$ such that $d_1 > \frac{2-3u_1^*}{\mu_{n_*}}$ and we have $\zeta_{n_*}(d_1) > 0 = d_2$, which leads to $D_{n_*} < 0$. This indicates that when $d_1 > 0$ and $d_2 = 0$, (u_1^*, v_1^*) is unstable.

Next, we suppose $d_1, d_2 > 0$. Note that $d_{1,n} \geq d_{1,n+1}$ and $d_{1,n} > \frac{2-3u_1^*}{\mu_n}$ for any $n \in \mathbb{N}$. Then, it follows from (2.14), (2.15) and (2.16) that if $d_1 \geq d_{1,1}$, then we have

(C1) $D_k > 0$ for $k \in \mathbb{N}$ provided that $d_2 > \zeta_1(d_1)$;
(C2) $D_1 < 0$ provided that $0 < d_2 < \zeta_1(d_1)$;

(C3) $D_1 = 0$ and $D_k > 0$ for $k \geq 2$ provided that $d_1 > d_{1,1}$ and $d_2 = \zeta_1(d_1)$;

(C4) $D_1 = D_2 = 0$ and $D_k > 0$ for $k \geq 3$ provided that $d_1 = d_{1,1}$ and $d_2 = \zeta_1(d_1)$;

while if $d_{1,n} \leq d_1 < d_{1,n-1}$ for some $n \geq 2$, then we find that

(C5) $D_k > 0$ for $k \in \mathbb{N}$ provided that $d_2 > \zeta_n(d_1)$;

(C6) $D_n < 0$ provided that $0 < d_2 < \zeta_n(d_1)$;

(C7) $D_n = 0$ and $D_k > 0$ for $k \neq n$ provided that $d_{1,n} < d_1 < d_{1,n-1}$ and $d_2 = \zeta_n(d_1)$;

(C8) $D_n = D_{n+1} = 0$ and $D_k > 0$ for $k \neq n, n+1$ provided that $d_1 = d_{1,n}$ and $d_2 = \zeta_n(d_1)$.

Therefore, by (2.10), (2.12), (C1), (C2), (C5) and (C6), we see that if $0 < d_2 < \zeta(d_1)$, then for some $n \in \mathbb{N}$, Λ_n has at least one root with positive real part, while if $d_2 > \zeta(d_1)$, then for any $n \in \mathbb{N}_0$, all roots of Λ_n have negative real parts, where $\zeta(d_1)$ is defined by (2.7). Furthermore, it follows from (2.10), (2.12), (C3) and (C7) that when $d_2 = \zeta_n(d_1)$ and $d_1 \neq d_{1,n}$, 0 is the root of Λ_n and other roots have negative real parts, while it follows from (2.10), (2.12), (C4) and (C8) that when $d_2 = \zeta_n(d_1)$ and $d_1 = d_{1,n}$, then 0 is the root of Λ_n and Λ_{n+1} and other roots have negative real parts. Finally, by (2.11), we have the following transversality condition

$$\frac{d\lambda_n(d_2)}{dd_2}\bigg|_{d_2=\zeta_n(d_1)} = -\frac{d_1\beta\mu_n^2 - \mu_n\left(\gamma - u_1^*(\beta+\gamma)\right)}{\beta T_n} < 0.$$

This completes the proof of the theorem. $\qquad\square$

Remark 2.1. Using (2.9), (2.10), (2.11) and the fact that $0 < u_1^* < \frac{2}{3}$, we obtain

$$\zeta_n(d_1) - d_1$$

$$= \frac{-d_1^2\mu_n^2\beta + d_1\mu_n(\gamma(1+\beta-\gamma)-u_1^*(\beta+\gamma))-\gamma(\beta-\gamma)(2-3u_1^*)}{d_1\beta\mu_n^2 - \mu_n(\gamma-u_1^*(\beta+\gamma))} < 0, \ n \in \mathbb{N},$$

which implies that $\zeta_n(d_1) < d_1$ for any $n \in \mathbb{N}$. Consequently, it follows from Theorem 2.3 that when $d_2 \geq d_1$ (i.e. The diffusive rate of predator is not smaller than that of prey), there is no diffusion-driven Turing instability.

Remark 2.2. We obtain a sufficient and necessary condition for the stability of the constant steady state (u_1^*, v_1^*) in Theorem 2.3. Unfortunately, the curve $d_2 = \zeta(d_1)$ is a piecewise function composed of $d_2 = \zeta_n(d_1)$, $n \in \mathbb{N}$, and the segment points are $(d_{1,n}, \zeta_n(d_{1,n}))$. By (2.6), it is easy to see that $d_{1,n} \geq d_{1,n+1}$ for each $n \in \mathbb{N}$, and $\lim\limits_{n\to\infty} d_{1,n} = 0$. Thus, we can not exactly depict the boundary curve $d_2 = \zeta(d_1)$ of the stable region when d_1 is close to zero. However, it is easy to determine that the envelope curve of Turing bifurcation curves $d_2 = \zeta_n(d_1)$, $n \in \mathbb{N}$ as follows:

$$C(d_1)$$

$$= \frac{d_1\gamma(\beta-\gamma)\left(-\gamma+u_1^*(\beta+\gamma)+2\beta(2-3u_1^*)-\sqrt{-4\beta\left(2-3u_1^*\right)\left(\gamma-u_1^*(\beta+\gamma)-\beta\left(2-3u_1^*\right)\right)}\right)}{\left(\gamma-u_1^*(\beta+\gamma)\right)^2}.$$
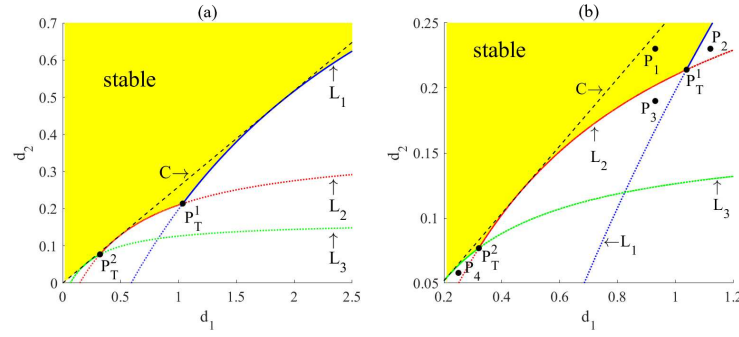
Figure 1. (a) illustrates the stability region of the positive steady state $(u_1^*, v_1^*) = (0.6173, 0.54)$ and (b) is the enlargement of (a) for $0.2 \le d_1 \le 1.2$ and $0.05 \le d_2 \le 2.5$. Here, C is the envelope curve, L_n, $n = 1, 2, 3$, are Turing bifurcation curves, and P_T^n, $n = 1, 2$, are Turing-Turing bifurcation points. In (b), $P_1 - P_4$ are chosen for numerical simulations.

This envelope curve $d_2 = C(d_1)$ is explicitly determined in the $d_1 - d_2$ plane. Thus, we can obtain a clear sufficient condition for the stability of the constant steady state (u_1^*, v_1^*), i.e. When $d_2 > C(d_1)$, the constant steady state (u_1^*, v_1^*) is locally asymptotically stable.

We consider $\Omega = (0, \ell\pi)$, and choose

$$\ell = 2, \ \alpha = 1.75, \ \beta = 2, \ \gamma = 0.5. \tag{2.17}$$

Since $\frac{4\beta(\beta-\gamma)}{27\gamma^2} = 1.7778$ and $\alpha_h = 0.375$, it is clear that $\gamma < \frac{2}{3}$, $\beta > \gamma$ and $\alpha_h < \alpha < \frac{4\beta(\beta-\gamma)}{27\gamma^2}$. Then, a direct computation gives $(u_1^*, v_1^*) = (0.6173, 0.54)$, $d_{1,1} = 1.0378$, $d_{1,2} = 0.3208$ and $d_{1,3} = 0.1573$. According to Theorem 2.3, we can depict the stability region and bifurcation curves for the positive steady state (u_1^*, v_1^*) in $d_1 - d_2$ plane. In fact, the boundary of the stable regions consists of Turing bifurcation curves $L_n : d_2 = \zeta_n(d_1)$, $n \in \mathbb{N}$, and we only illustrate three of them in Figure 1.

Besides, the envelope curve $C : d_2 = C(d_1)$ intersects L_1, L_2 and L_3 respectively at $(1.8516, 0, 4797)$, $(0.4629, 0.1199)$ and $(0.2057, 0.0533)$. In Figure 1(a), L_1 and L_2 intersect at $P_T^1 = (d_{1,1}, \zeta_1(d_{1,1}))$, L_2 and L_3 intersect at $P_T^2 = (d_{1,2}, \zeta_2(d_{1,2}))$; in Figure 1(b), $P_1 - P_4$ are chosen for numerical simulations in Section 4, where

$$P_1 = (0.93, 0.23), \ P_2 = (1.12, 0.23), \ P_3 = (0.93, 0.19), \ P_4 = (0.25, 0.058). \tag{2.18}$$

Notice that for the point P_1 between the boundary curve $d_2 = \zeta(d_1)$ and the envelope curve $d_2 = C(d_1)$, the positive steady state (u_1^*, v_1^*) is still asymptotically stable. For the points $P_j, j = 2, 3, 4$ under the boundary curve $d_2 = \zeta(d_1)$, the positive steady state (u_1^*, v_1^*) is unstable and the nonconstant positive steady states emerge near (u_1^*, v_1^*).

3. Nonexistence of nonconstant positive steady states

In this section, we apply similar arguments as in [4, 20, 23] and discuss the nonconstant steady states of system (1.3).

Theorem 3.1. *If either $\beta \leq \gamma$, or $\beta > \gamma$ and $d_1, d_2 > d_*$, where*

$$d_* = \max\left\{ \frac{1}{\mu_1}\left(1 + \frac{\alpha}{2} + \frac{\beta^3}{2\alpha^2\gamma^2}\right), \frac{1}{\mu_1}\left(\beta - \gamma + \frac{\alpha}{2} + \frac{\beta^3}{2\alpha^2\gamma^2}\right)\right\}, \qquad (3.1)$$

then system (1.3) *admits no nonconstant positive steady states.*

Proof. If $\beta \leq \gamma$, then it follows from Theorem 2.2 that system (1.3) admits only constant steady states. Next, we focus on $\beta > \gamma$. Notice that the steady state of system (1.3) is also the solution of

$$
\begin{cases}
-d_1\Delta u = u(1 - u) - \frac{\alpha uv^2}{1+uv}, & x \in \Omega, \\[2mm]
-d_2\Delta v = \frac{\beta uv^2}{1+uv} - \gamma v, & x \in \Omega, \\[2mm]
\frac{\partial u}{\partial n} = \frac{\partial v}{\partial n} = 0, & x \in \partial\Omega.
\end{cases}
\qquad (3.2)
$$

Assume that $(u(x), v(x))$ is a positive solution of system (3.2). Since $u, v > 0$, we have $\hat{u}, \hat{v} > 0$, where

$$\hat{u} = \frac{1}{|\Omega|}\int_\Omega u\,dx, \ \hat{v} = \frac{1}{|\Omega|}\int_\Omega v\,dx.$$

In system (3.2), we multiply the equation of u by $u - \hat{u}$ and the equation of v by $v - \hat{v}$ and integrate these two equations to obtain

$$d_1 \int_\Omega |\nabla(u - \hat{u})|^2 dx$$

$$= \int_\Omega (u - \hat{u})\left(u(1-u) - \frac{\alpha uv^2}{1+uv}\right) dx$$

$$= \int_\Omega (u - \hat{u})\left(u(1-u) - \hat{u}(1-\hat{u}) + \frac{\alpha \hat{u}\hat{v}^2}{1+\hat{u}\hat{v}} - \frac{\alpha uv^2}{1+uv}\right) dx$$

$$= \int_\Omega (u - \hat{u})^2(1 - u - \hat{u})dx + \alpha \int_\Omega (u - \hat{u})\left(\frac{\hat{u}\hat{v}^2}{1+\hat{u}\hat{v}} - \frac{u\hat{v}^2}{1+u\hat{v}} + \frac{u\hat{v}^2}{1+u\hat{v}} - \frac{uv^2}{1+uv}\right) dx$$

$$= \int_\Omega (u - \hat{u})^2(1 - u - \hat{u})dx - \alpha \int_\Omega \frac{(u-\hat{u})^2\hat{v}^2}{(1+\hat{u}\hat{v})(1+u\hat{v})}dx - \alpha \int_\Omega \frac{(u-\hat{u})(v-\hat{v})(uv+u\hat{v}+u^2v\hat{v})}{1+uv+u\hat{v}+u^2v\hat{v}}dx$$

$$\leq \int_\Omega (u - \hat{u})^2 dx - \alpha \int_\Omega \frac{(u-\hat{u})(v-\hat{v})(uv+u\hat{v}+u^2v\hat{v})}{1+uv+u\hat{v}+u^2v\hat{v}}dx$$

$$\leq \int_\Omega (u - \hat{u})^2 dx + \frac{\alpha}{2}\int_\Omega (u - \hat{u})^2 dx + \frac{\alpha}{2}\int_\Omega (v - \hat{v})^2 dx,$$

and

$$d_2 \int_\Omega |\nabla(v - \hat{v})|^2 dx$$

$$= \int_\Omega (v - \hat{v}) \left(\frac{\beta u v^2}{1+uv} - \gamma v \right) dx$$

$$= \int_\Omega (v - \hat{v}) \left(\frac{\beta u v^2}{1+uv} - \frac{\beta \hat{u} \hat{v}^2}{1+\hat{u}\hat{v}} + \gamma \hat{v} - \gamma v \right) dx$$

$$= -\gamma \int_\Omega (v - \hat{v})^2 dx + \beta \int_\Omega (v - \hat{v}) \left(\frac{uv^2}{1+uv} - \frac{u\hat{v}^2}{1+u\hat{v}} + \frac{u\hat{v}^2}{1+u\hat{v}} - \frac{\hat{u}\hat{v}^2}{1+\hat{u}\hat{v}} \right) dx$$

$$= -\gamma \int_\Omega (v - \hat{v})^2 dx + \beta \int_\Omega \frac{(v-\hat{v})^2 (uv + u\hat{v} + u^2 v\hat{v})}{1+uv+u\hat{v}+u^2 v\hat{v}} dx + \beta \int_\Omega \frac{\hat{v}^2 (u-\hat{u})(v-\hat{v})}{(1+\hat{u}\hat{v})(1+u\hat{v})} dx$$

$$\leq (\beta - \gamma) \int_\Omega (v - \hat{v})^2 dx + \beta \int_\Omega \frac{\hat{v}^2 (u-\hat{u})(v-\hat{v})}{(1+\hat{u}\hat{v})(1+u\hat{v})} dx$$

$$\leq (\beta - \gamma) \int_\Omega (v - \hat{v})^2 dx + \frac{\beta}{2} \int_\Omega \hat{v}^2 (u - \hat{u})^2 dx + \frac{\beta}{2} \int_\Omega \hat{v}^2 (v - \hat{v})^2 dx,$$

respectively. It follows from the maximum principle [10] that

$$u \leq 1. \tag{3.3}$$

Furthermore, integrating the equations of system (3.2) gives

$$\alpha \gamma \int_\Omega v \, dx = \beta \int_\Omega u(1 - u) \, dx,$$

which, together with (3.3), implies

$$\hat{v} \leq \frac{\beta}{\alpha \gamma}. \tag{3.4}$$

Using (3.4) and the Poincaré inequality, we see that

$$d_1 \int_\Omega |\nabla(u - \hat{u})|^2 dx + d_2 \int_\Omega |\nabla(v - \hat{v})|^2 dx$$

$$\leq \left(1 + \frac{\alpha}{2} + \frac{\beta^3}{2\alpha^2\gamma^2} \right) \int_\Omega (u - \hat{u})^2 dx + \left(\beta - \gamma + \frac{\alpha}{2} + \frac{\beta^3}{2\alpha^2\gamma^2} \right) \int_\Omega (v - \hat{v})^2 dx$$

$$\leq \frac{1}{\mu_1} \left(1 + \frac{\alpha}{2} + \frac{\beta^3}{2\alpha^2\gamma^2} \right) \int_\Omega |\nabla(u - \hat{u})|^2 dx + \frac{1}{\mu_1} \left(\beta - \gamma + \frac{\alpha}{2} + \frac{\beta^3}{2\alpha^2\gamma^2} \right) \int_\Omega |\nabla(v - \hat{v})|^2 dx.$$

Hence, we can conclude that when $\beta > \gamma$ and $d_1, d_2 > d_*$, system (1.3) admits only positive nonconstant steady states. This completes the proof. $\square$

4. Numerical simulations

Numerical simulations are conducted and $\Omega = (0, \ell\pi)$ is considered in this section. We first take the parameters as in (2.17) and illustrate the solutions of system (1.3) for $P_1 - P_4$, which are defined by (2.18) and shown in Figure 1(b). Figures 2 (a) and (e) describe the stable constant positive steady state $(u_1^*, v_1^*) = (0.6173, 0.54)$; Figures 2 (b) and (f) illustrate the nonconstant positive steady state shaped like $\cos \frac{1}{2}x$; (c) and (g) depict the nonconstant positive steady state shaped like $\cos x$; Figures 2 (d) and (h) show the nonconstant positive steady state shaped like $\cos \frac{3}{2}x$.
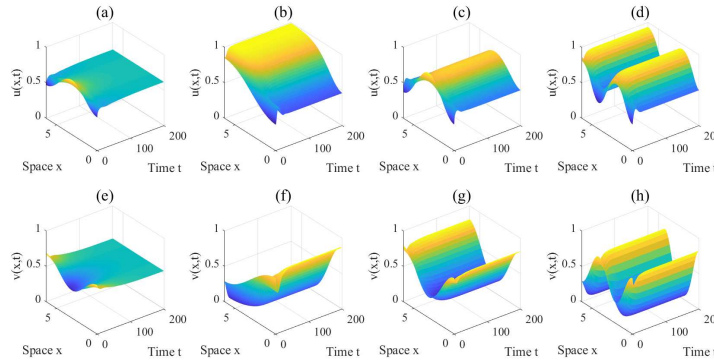
Figure 2. (a) and (e) show the solution for P_1; (b) and (f) show the solution for P_2; (c) and (g) show the solution for P_3; (d) and (h) show the solution for P_4. Here, $P_1 - P_4$ are defined by (2.18) and shown in Fig.1(b).

Then, it follows from Theorem 2.1 that for P_1, $E_1(1,0)$ and $(u_1^*, v_1^*) = (0.6173, 0.54)$ are both locally asymptotically stable, while for $P_2 - P_4$, $E_1(1,0)$ and the stable nonconstant positive steady states coexist. We note that which steady state the solution will converge to depends on the choice of initial conditions.

Take $\alpha = 0.063$, $\beta = 0.75$, $\gamma = 0.5$ and $\ell = 5$. Numerical computation shows that $(u_1^*, v_1^*) = (0.3632, 5.5067)$, $(u_2^*, v_2^*) = (0.8952, 2.2342)$ and $\frac{\gamma(1+\beta-\gamma)}{\beta+\gamma} = 0.5$. Thus, we have $u_1^* < \frac{\gamma(1+\beta-\gamma)}{\beta+\gamma}$. It follows from (2.9) that (u_1^*, v_1^*) is unstable. When $d_1 = 1$ and $d_2 = 175$, there exists a heteroclinic orbit between the unstable nonconstant steady state shaped like $\cos\frac{1}{5}x$ and the stable steady state $E_1(1,0)$, as depicted in Figure 3.
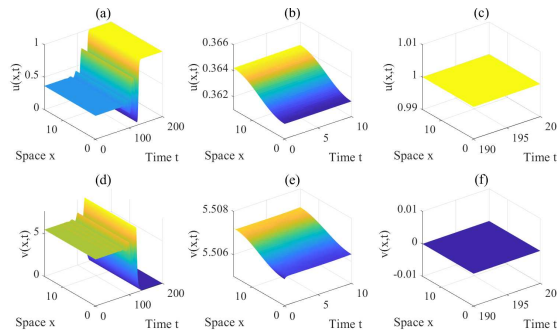

Figure 3. (a) and (d) show that the solution with an initial spatial mode like $\cos\frac{1}{5}x$ eventually converges to $E_1(1,0)$; (b) and (e) are the short-term behaviour of (a) and (d), respectively, while (c) and (f) are the long-term behaviour of (a) and (d), respectively.

5. Conclusion and discussion

Considering the random movement of the species in space, we introduce the self-diffusion into the predator-prey model with hunting cooperation proposed by Conser *et al.* [5]. We investigate diffusion-driven Turing instability and derive the conditions

for Turing bifurcation to occur. Moreover, we take $\Omega = (0, \ell\pi)$ and depict Turing bifurcation curves and stability region in the plane of the diffusion coefficients d_1 and d_2. It is well known that Turing instability usually occurs when the diffusive rate of predator is larger than that of prey and much of the existing investigation on Turing instability has focused on this case. In system (1.3), when the diffusive rate of predator is larger than that of prey, Turing instability can not occur due to the functional response involving hunting cooperation (1.1). Similar results are also found in [3, 16, 21, 22].

When there is diffusion, we show that the semi-trivial steady state $E_1(1, 0)$ remains locally asymptotically stable. Therefore, it is possible for the semi-trivial steady state $E_1(1, 0)$ and the constant/nonconstant positive steady state to coexist. More specifically, if the diffusive rate of predator is larger than the critical value $\zeta(d_1)$ defined by (2.7), then both the semi-trivial steady state and the constant positive steady state are locally asymptotically stable, while if the diffusive rate of predator is smaller than $\zeta(d_1)$, the semi-trivial steady state and the nonconstant positive steady state may coexist. Numerical simulations support these results and nonconstant positive steady states with different spatial profiles are observed. By the Lyapunov functional method, we demonstrate the global attractivity of $E_1(1, 0)$ for $\beta \leq \gamma$. Unfortunately, we can not extend this result to include the conditions $\beta > \gamma$ and $\alpha > \frac{4\beta(\beta-\gamma)}{27\gamma^2}$, under which $E_1(1, 0)$ is globally asymptotically stable in the model without diffusion.

We also investigate the conditions under which nonconstant positive steady states don't exist. From Theorem 3.1, we know that model (1.3) possesses no nonconstant positive steady states if either $\beta \leq \gamma$, or $\beta > \gamma$ and d_1, d_2 are both larger than the critical value d_* defined by (3.1). In addition, numerical simulations suggest that for sufficient large d_2, the nonconstant positive steady state is unstable and evolves into the the semi-trivial steady state $E_1(1, 0)$ as time increases. This is because if the predator spreads very quickly, the prey will be quickly consumed and then the predator will be ultimately extinct due to lack of enough food.

References

[1] M. T. Alves and F. M. Hilker, *Hunting cooperation and Allee effects in predators*, Journal of Theoretical Biology, 2017, 419, 13–22.

[2] L. Berec, *Impacts of foraging facilitation among predators on predator-prey dynamics*, Bulletin of Mathematical Biology, 2010, 72(1), 94–121.

[3] F. Capone, M. F. Carfora, R. De Luca and I. Torcicollo, *Turing patterns in a reaction-diffusion system modeling hunting cooperation*, Mathematics and Computers in Simulation, 2019, 165, 172–180.

[4] S. Chen, J. Wei and J. Yu, *Stationary patterns of a diffusive predator-prey model with Crowley-Martin functional response*, Nonlinear Analysis: Real World Applications, 2018, 39, 33–57.

[5] C. Cosner, D. DeAngelis, J. Ault and D. Olson, *Effects of spatial grouping on the functional response of predators*, Theoretical Population Biology, 1999, 56(1), 65–75.

[6] S. R. Dunbar, *Traveling waves in diffusive predator-prey equations: periodic orbits and point-to-periodic heteroclinic orbits*, SIAM Journal on Applied Mathematics, 1986, 46(6), 1057–1078.

[7] J. Huang, G. Lu and S. Ruan, *Existence of traveling wave solutions in a diffusive predator-prey model*, Journal of Mathematical Biology, 2003, 46(2), 132–152.

[8] W. Li and S. Wu, *Traveling waves in a diffusive predator-prey model with holling type-III functional response*, Chaos, Solitons & Fractals, 2008, 37(2), 476–486.

[9] C. Lin, W. Ni and I. Takagi, *Large amplitude stationary solutions to a chemotaxis system*, Journal of Differential Equations, 1988, 72(1), 1–27.

[10] Y. Lou and W. Ni, *Diffusion, self-diffusion and cross-diffusion*, Journal of Differential Equations, 1996, 131(1), 79–131.

[11] W. Ni and M. Wang, *Dynamics and patterns of a diffusive Leslie-Gower prey-predator model with strong Allee effect in prey*, Journal of Differential Equations, 2016, 261(7), 4244–4274.

[12] K. Ryu and W. Ko, *Asymptotic behavior of positive solutions to a predator-prey elliptic system with strong hunting cooperation in predators*, Physica A, 2019, 531, Article ID 121726.

[13] K. Ryu, W. Ko and M. Haque, *Bifurcation analysis in a predator-prey system with a functional response increasing in both predator and prey densities*, Nonlinear Dynamics, 2018, 94(3), 1639–1656.

[14] T. Singh and S. Banerjee, *Spatial aspect of hunting cooperation in predators with Holling type II functional response*, Journal of Biological Systems, 2018, 26(4), 511–531.

[15] T. Singh, R. Dubey and V. N. Mishra, *Spatial dynamics of predator-prey system with hunting cooperation in predators and type I functional response*, AIMS Mathematics, 2020, 5(1), 673–684.

[16] D. Song, C. Li and Y. Song, *Stability and cross-diffusion-driven instability in a diffusive predator-prey system with hunting cooperation functional response*, Nonlinear Analysis: Real World Applications, 2020, 54, Article ID 103106.

[17] D. Song, Y. Song and C. Li, *Stability and turing patterns in a predator-prey model with hunting cooperation and allee effect in prey population*, International Journal of Bifurcation and Chaos, 2020, 30(9), Article ID 2050137.

[18] Y. Song, T. Zhang and Y. Peng, *Turing-Hopf bifurcation in the reaction-diffusion equations and its applications*, Communications in Nonlinear Science and Numerical Simulation, 2016, 33, 229–258.

[19] Y. Song and X. Zou, *Bifurcation analysis of a diffusive ratio-dependent predator-prey model*, Nonlinear Dynamics, 2014, 78(1), 49–70.

[20] J. Wang, J. Wei and J. Shi, *Global bifurcation analysis and pattern formation in homogeneous diffusive predator-prey systems*, Journal of Differential Equations, 2016, 260(4), 3495–3523.

[21] D. Wu and M. Zhao, *Qualitative analysis for a diffusive predator-prey model with hunting cooperative*, Physica A, 2019, 515, 299–309.

[22] S. Yan, D. Jia, T. Zhang and S. Yuan, *Pattern dynamics in a diffusive predator-prey model with hunting cooperations*, Chaos, Solitons & Fractals, 2020, 130, Article ID 109428.

[23] F. Yi, J. Wei and J. Shi, *Bifurcation and spatiotemporal patterns in a homogeneous diffusive predator-prey system*, Journal of Differential Equations, 2009, 246(5), 1944–1977.

[24] X. Zhang and H. Zhu, *Dynamics and pattern formation in homogeneous diffusive predator-prey systems with predator interference or foraging facilitation*, Nonlinear Analysis: Real World Applications, 2019, 48, 267–287.